ROS

RESEARCH ARTICLES

Stress-Generated Free Radicals Detected by Electron Paramagnetic Resonance Spectroscopy with Nitrone Spin Trap in *Vicia faba* Root

Shweta Kaur[1], Smita Sundaram[1,2], Ramovatar Meena[1], and Paulraj Rajamani[1]

[1]School of Environmental Sciences, Jawaharlal Nehru University, New Delhi-110 067, India; [2]Advance Instrumentation Research Facility, Jawaharlal Nehru University, New Delhi-110 067, India

Correspondence: paulrajr@hotmil.com (P.R.)

Kaur S et al. Reactive Oxygen Species 5(14):134–144, 2018; ©2018 Cell Med Press
http://dx.doi.org/10.20455/ros.2018.823
(Received: October 21, 2017; Revised: December 6, 2017; Accepted: December 6, 2017)

ABSTRACT | Electron paramagnetic resonance (EPR) spectroscopy is a promising technique for detection and quantification of short-lived free radicals in biological systems. In the present investigation, root of *Vicia faba* seedlings were subjected to 0.5 mM (T1) and 1 mM (T2) sodium azide (NaN_3) in hydroponic medium. The stress-generated free radicals (superoxide and hydroxyl free radicals) in the root tips of the seedlings were analyzed by EPR spectroscopy using 5,5-dimethyl-1-pyrroline-*N*-oxide (DMPO) nitrone spin. Single cell gel electrophoresis (comet assay) and mitotic index along with the spectrophotometric measurement of the two major antioxidant enzymes, namely, superoxide dismutase (SOD) and catalase (CAT), in combination with analysis of lipid peroxidation product, malondialdehyde (MDA), were done to validate the EPR results. Data obtained from comet assay of root tip cells revealed significant increase in the olive moment in T1 and T2 as compared to control. Decreased mitotic index in T2 (60.63 ± 7.74%) as compared to control (88.23 ± 1.01%) in these cells as a consequence of increased reactive oxygen species (ROS) was depicted. Furthermore, the decrease in the activity of major antioxidant enzymes, SOD and CAT justified the intensified DMPO-OH specific peaks in T2 as compared to control obtained in the EPR spectra. The results establish that EPR spectroscopy can be used successfully at room temperature to monitor changes in the production of free radicals (combined superoxide and hydroxyl free radicals) in plant tissues using DMPO as a spin trap.

KEYWORDS | 5,5-Dimethyl-1-pyrroline-*N*-oxide; Electron paramagnetic resonance; Reactive oxygen species; Sodium azide; Spin-trapping; *Vicia faba*

ABBREVIATIONS | ATP, adenosine triphosphate; CAT, catalase; DMPO, 5,5-dimethyl-1-pyrroline-*N*-oxide; EPR, electron paramagnetic resonance; MDA, malondialdehyde; NBT, nitro blue tetrazolium chloride; NMPA, normal melting point agarose; ROS, reactive oxygen species; SOD, superoxide dismutase; TCA, trichloroacetic acid

CONTENTS

1.INTRODUCTION

EPR is an instant, sensitive, and non-invasive technique for detection and quantification of free radicals in biological and environmental samples [1–3]. This technique is used for detection of paramagnetic substances, such as free radicals, transition metals, and irregular crystal structures carrying unpaired electrons. The unpaired electrons belonging to transition metals and crystal structures in non-biological samples are relatively stable and therefore easily detected by EPR. Most of the free radicals generated in vivo are highly reactive and possess a half-life in the range of nanoseconds to milliseconds, which are difficult to be detected directly by EPR [4]. To resolve this, various spin traps have been designed which react with free radicals to produce comparatively stable spin trap adducts suitable for the detection by EPR. One of the most popular nitrone spin traps is 5,5-dimethyl-1-pyrroline-*N*-oxide (DMPO). It is a nitrone compound with diamagnetic property and particularly useful for identifying oxygen-centered free radicals, such as superoxide and hydroxyl radicals, and it can also be applied to detect carbon-, nitrogen-, and sulfur-centered radicals [5, 6]. This spin trap has noticeable inactive redox status, so it can easily be used to detect superoxide and hydroxyl free radicals produced inside plant and animal tissues. In biological samples, DMPO-superoxide adduct (DMPO-OOH, $t_{1/2}$ = 45–60 s) spontaneously decays into comparatively longer half-life DMPO-hydroxyl adduct (DMPO-OH, $t_{1/2}$ = 23 min) [7]. Due to conversion of DMPO-superoxide adduct into DMPO-hydroxyl adduct within few seconds, the DMPO-hydroxyl adduct remains the only product which is detectable even after 15–20 min of incubation of plant tissues with the spin trap [8]. Therefore, both the superoxide and the hydroxyl radicals produced inside living tissues are detected by DMPO-OH specific EPR spectrum. As such, the spectrum generated by this spin trap is incapable of distinguishing the superoxide free radicals from the hydroxyl free radicals when detected after a considerable time. Although by using this spin trap we cannot measure the absolute quantity of the superoxide and hydroxyl radicals separately, EPR is very useful in combined monitoring of the two-free radicals for multiple sample comparative analyses.

It is a very common practice to treat model plants and animals with chemical mutagens to understand the effects and the mechanisms of induced mutations. Sodium azide (NaN_3) has been found to be mutagenic to various bacterial strains, plants, and animals, and cause stress when used in an excess amount. Increased genetic variability, enhanced stress tolerance, and crop yields in crops (e.g., barley, wheat, groundnut, tomato, chickpea) have been shown to be induced by NaN_3 treatment [9–14]. L-Azidoalanine, formed by the action of the enzyme lyase on *O*-acetylserine and azide is responsible for the mutagenic effects (point mutation) induced by NaN_3 [15–17]. Azide-induced inhibition of many enzymes like SOD, CAT, peroxidases, and cytochrome oxidase has been documented [18].

To assess the toxicity of environmental pollutants, higher plant species such as *Allium cepa, Zea mays, Tradescantia, Nicotiana tabacum, Hordeum vulgare, and Vicia faba* have been widely used [19–22]. Among them, *Vicia faba* is easy to grow with relatively high yield potential and has small number of chromosomes (2 n = 12). Thus, *Vicia faba* is a useful plant model for understanding the effects of various environmental factors on plants [23].

In the present study, *Vicia faba* was selected as a prototype for the detection of NaN_3-induced free radicals in their root tip using EPR technology. Activities of major antioxidative enzymes were assayed to examine the enhanced generation of free radicals. Furthermore, genotoxic and cytotoxic assays were performed to evaluate the effects of NaN_3 on root cell's integrity and performance. Results of the present study established the successful usage of EPR spectroscopy at room temperature.

2. MATERIALS AND METHODS

Analytical grade DMPO (Catalogue No. 92688) was procured from Sigma-Aldrich (St. Louis, MO, USA). All other chemicals were purchased from Sigma-Aldrich or Merck (Darmstadt, Germany).

2.1. Sample Preparation and Treatment

Seeds of *Vicia faba* were kindly provided by the National Bureau of Plant Genome Research (NBPGR), Pusa, New Delhi, India. These seeds were grown hydroponically in ½ strength Hoagland nutrient medium. Briefly, seeds were surface sterilized for 30 s with 0.1% $HgCl_2$ and rinsed several times with distilled water. For germination, the seeds were soaked in distilled water overnight and kept in a seed germinator (Thermotech, India) between two germinating sheets that were rolled and kept vertically for five days. Germination was carried out in dark at 23°C (± 0.5°C). The germinated seedlings with a radical length of 20–30 mm were kept in various pots supplied with 100 ml of half-strength Hoagland solution, grown hydroponically, in a plant growth chamber. Cool-white fluorescent light was provided to the plants to generate artificial light (photon flux density of 200 µmol $m^{-2}s^{-1}$) for 12 h photoperiods. Seedling roots were continually aerated using an aeration pump.

NaN_3 solution in ½ strength Hoagland solutions was prepared at concentrations of 0.5 mM (T1) and 1 mM (T2) for treatment while control seedlings were similarly grown in ½ strength Hoagland medium. Detection of free radicals was carried out after 24 h of treatment.

2.2. EPR Spectroscopy

EPR measurements were carried out in a Bruker EMX Micro X spectrometer. The following conditions were set for the measurement: Sweep width, 200.83; modulation amplitude, 4.0 G; microwave power, 16 mW; temperature, 298 K; conversion time, 40 ms; and time constant, 163.84 ms. Treated samples were chopped and suspended in 100 mM DMPO. Samples were loaded in sealed quartz capillary tubes and transferred to the EPR cavity to obtain spectra. For each sample, a 2D spectrum was recorded by Bruker e-Scan EPR. Spectrometric quantitation of EPR spectra and baseline correction were done using the Bruker WinEPR data processing software.

2.3. Nitro Blue Tetrazolium Chloride Assay

For detecting differential superoxide localization in the root tips, the method of Del Carmen De Pinto et al. [24] was followed. *Vicia* roots of approximately 50 mm long were excised from the tips for infiltration in 0.1 mM nitro blue tetrazolium chloride (NBT) solution for 5 h. Differential appearance of purple color in the roots was recorded.

2.4. SOD Assay

SOD activity was assayed by monitoring the inhibition of photochemical reduction of NBT by the method described by Giannopolitis and Ries [25]. For preparation of crude enzyme extract, plant tissues were weighed, and 25–100 mg tissues were homogenized (Remi Electrotechnik, India) at 7000 rpm in 500 µl ice cold extraction buffer (100 mM potassium phosphate buffer and 0.1 mM Na_2EDTA, pH 7.8). The homogenate was centrifuged at 15,000 rpm in a refrigerated centrifuge (Eppendorf centrifuge 5418R, Germany) at 4°C for 30 min. The supernatant was stored at 4°C until its further use for the assay, and the sample was used for the experiments within 10 h. For preparation of reaction mixture, 13 mM methionine, 63 µM NBT, 50 mM phosphate buffer

(pH 7.8), 100 µL enzyme extract (or extraction buffer as blank), and 1.3 µM riboflavin were added in a glass test tube in the same order to prepare a final 3 ml reaction mixture. Reaction mixtures were retained in glass test tubes and illuminated by a cool lamp (Osram, L32W/765C) for 15 min. Optical density was measured by a spectrophotometer (Shimadzu UV-1800, Kyoto, Japan) for the determination of initial rate of reaction at 560 nm. The reaction mixture containing 100 µl of extraction buffer in place of 100 µl enzyme extract served as the blank. Percentage inhibition was calculated using the following formula: Inhibition% (I%) = [Increase in absorbance of blank – Increase in absorbance of sample] ÷ [Increase in absorbance of blank] × 100.

In general, with the crude enzyme extracts, 70% is the maximum achievable inhibition, while the pure SOD can give as high as 95% of inhibition [26]. Samples were appropriately diluted with buffer to achieve 20–70% inhibition. One unit of SOD is defined as the amount of enzyme that inhibits 50% of NBT photo reduction under a given reaction condition. Specific SOD activity was expressed as unit SOD per mg protein. Protein in the crude extract was determined by the Bradford method [27].

2.5. CAT Assay

CAT assay was performed to detect H_2O_2 concentration in the plant samples by the method as described by Sinha [28]. About 100 mg tissue samples were homogenized at 15,000 rpm in 1 ml cold extraction buffer (50 mM potassium phosphate buffer, pH 7.0) for 10 min. The crude extract was diluted at least 1,000 times in 0.5% bovine serum albumin (prepared in 10 mM phosphate buffer). Two ml of dichromate/acetic acid (D/A) reagent were prepared in advance. Four ml of 0.2 M H_2O_2 and 5 ml of 10 mM phosphate buffer were kept in one flask. To start the reaction, 1 ml of prepared plant extract was added in the flask and mixed gently. After that, 1 ml reaction mixture was added immediately into previously prepared test tube containing 2 ml of the D/A reagent. After every 1 min, 1 ml of reaction mixture was added in new test tubes containing 2 ml of the D/A reagent. All the test tubes were kept in a water bath maintained at 100ºC for 10 min. After cooling down all the test tube mixtures were centrifuged at 15,000 rpm at 4ºC for 10 min and the respective supernatant was used to record the absorbance at 570 nm by a spectrophotometer for the residual H_2O_2 concentration in the reaction mixtures. H_2O_2 (10, 100, and 200 µM) was used to prepare a standard H_2O_2 curve. From the standard H_2O_2 curve, for each sample residual H_2O_2 concentration at various time intervals in the reagent mixture was plotted. Velocity constant K was calculated using the following formula: $K= 1/T \log_{10} (S_o/S_t)$, where, S_o = initial residual H_2O_2 in the reaction mixture; S_t = residue H_2O_2 in the reaction mixture after time t. Graph K (velocity constant) versus T was plotted and extrapolated up to T = 0, to find out initial velocity constant for each sample. The specific catalase activity was expressed kat/g protein.

2.6. Lipid Peroxidation Assay

MDA content was measured as described by Dhindsa et al. [29]. Root samples were weighed, homogenized in 1 ml of 0.1% trichloroacetic acid (TCA). The homogenate was centrifuged at 15,000 rpm for 5 min at 4°C. An aliquot of 300 µl was mixed with 1.2 ml of 0.5% thiobarbituric acid (TBA) prepared in 20% TCA. Reagent mixture was incubated at 95°C for 30–45 min. The reaction was stopped by putting the reagent mixture in an ice bath. Subsequently, the samples were again centrifuged at 15,000 rpm for 10 min at room temperature. Absorbance of the supernatant was measured at 532 and 600 nm (subtracted to remove non-specific absorbance). MDA concentration was determined using the extinction coefficient of 155 $mM^{-1}cm^{-1}$.

2.7. Mitotic Index Assay

Root tips (1–2 mm long) were transferred to ice-cold fixative (methanol: acetic acid in 3:1 ratio) and kept at 4ºC overnight and subsequently are stored in 70% ethanol at 4ºC. Root tips (2 to 3) were hydrolyzed in 1–2 ml HCl (1 N) solution at 60ºC for 8–10 min. Root tips were blotted dry on a paper towel and placed on a clean microscope slide. A drop of acetocarmine was applied on the root tip and the tip was chopped into smaller sections for getting single layer of cells. A cover slip was placed on the slide, slowly lowering onto the stain to prevent bubble formation. At least 4 times folded paper towel was wrapped on the slide and the slide was pressed with thumb on the area of the root tip to prepare squash. The slide was heated over a burner slightly. A light microscope was used to detect dividing cells at various stages (pro-

phase, metaphase, anaphase, and telophase) of cell division.

2.8. Single-Cell Gel Electrophoresis (Comet Assay)

Alkaline single-cell gel electrophoresis of *Vicia faba* roots was performed as per the method described by Gichner and Plewa [30], with minor modifications. For the base slide preparation, 1% normal melting point agarose was maintained at 60°C in a water bath in a 50 ml falcon tube. The clean dried frosted slides were dipped in the agarose for 2 s and then kept vertically. The backside of the slide was wiped with tissue paper and kept at room temperature for drying. Nuclei isolation buffer (NIB) was prepared according to Galbraith et al. [31]. Plant leaf nuclei were isolated by chopping. In brief, a single fresh leaf of approximately 50 mg was kept in a petri plate containing 1–2 ml of NIB at 4°C. The plate was kept slightly tilted on ice. Each leaf was chopped using a fresh sharp razor blade (one edged) releasing nuclei in the buffer. The nuclei suspension was filtered through four-layered cheesecloth followed by a nylon mesh of 40 µm. Immediately after the preparation of nuclei suspension, 300 µl of nuclear suspension was mixed with 600 µl of 0.75% low melting point agarose to make final 0.5% ow melting point agarose and 90 µl of the prepared agarose was spread on the base slide by placing a coverslip gently on it. At least 5 slides were prepared for each treatment. The slides were kept on ice for 5 min and then the cover slip was removed gently. Lysis buffer was prepared by adding 2.5 M NaCl, 100 mM Na-EDTA, and 10 mM Tris buffer (pH 10). Just before use, 1% Triton X-100 was added. Lysis buffer was dropped onto the slides with the help of a Pasteur pipette and the slides were kept for 1 h at 4°C in dark. After this, the slides were kept for unwinding in electrophoretic buffer (300 mM NaOH and 1 mM Na-EDTA, pH > 13) for 30 min, followed by electrophoresis at 25 V and 300 mA for 10 min. After electrophoresis, the slides were rinsed 3 times with 0.4 M Tris buffer (pH = 7.5) each for 5 min. Slides were stained with 60 µl ethidium bromide (EtBr) (20 µg/ml), dipped in ice-cold distilled water to remove any excess EtBr, and covered with a cover slip. Slides were visualized by a fluorescent microscope using a 568 nm filter. For each slide, at least 50 cells were analyzed for various comet parameters using the image analysis software Open Comet version v1.3 (www.comerbio.org).

2.9. Statistical Analysis

All experimental data were expressed as mean ± standard error of three replicates. In all the experiments except the Comet assay, analysis of variance followed by Tukey's post-hoc test was used for accessing statistical differences between the control and treated groups. Nonparametric Kruskal–Wallis test followed by Dunn's multiple comparison was applied for the analysis of tail moments in Comet assay. All the analyses were done by GraphPad Prism software (La Jolla, CA, USA), and $p < 0.05$, $p < 0.01$, and $p < 0.001$ were used to determine statistically significant, very significant, and very, very significant data, respectively, in the analyses.

3. RESULTS

3.1. NBT Test to Visualize Superoxide in *Vicia* Root

To determine whether root cells possessed the altered superoxide level, NBT histochemical staining method was applied. It revealed the alteration in superoxide levels in treated groups (T1 and T2) versus control group (C). NBT reacts with superoxide to form a colored precipitate. The maximum color (dark purple) was developed in T2, followed by T1 and C (**Figure 1**).

3.2. Detection of Free Radicals in Root Tip by EPR Spectroscopy

As the root tips were found to be the most affected part in the NBT test, tip region approximately 2 mm long were further used to detect and quantify the combined production of superoxide and hydroxyl free radicals by EPR spectroscopy using DMPO spin trap. As the EPR spectra of the DMPO-radical adduct depicted, the higher dose of NaN_3 in T2 resulted in six prominent peaks (**Figure 2**, peaks no. 1–6) with a greater intensity as compared to the lower dose (T1) and control (C) (**Figure 2**). The middle prominent peak in all the three spectra (C, T1 and T2) represents a *g* value equal to 2.006 characteristic for the DMPO-OH adduct. The relative free radical concentration (combined concentrations of superoxide and hydroxyl free radicals) inside the root tips can be measured by calculating the increase in the central

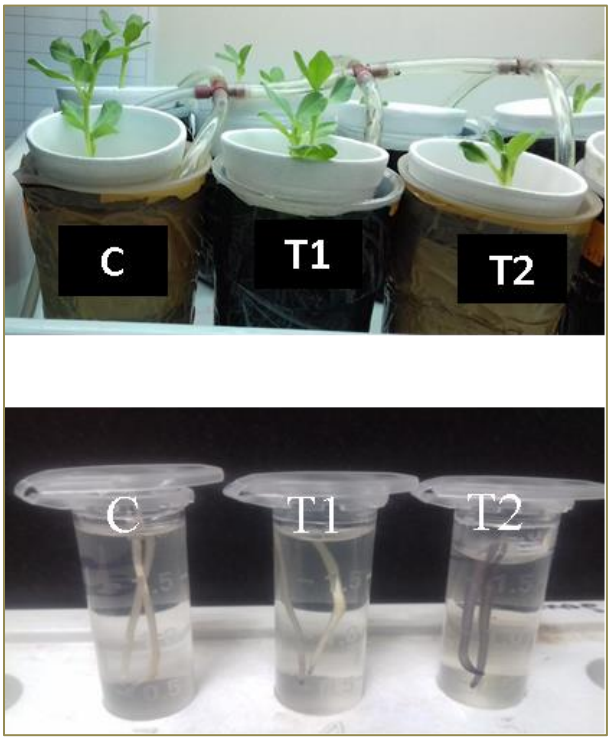

FIGURE 1. Effects of NaN_3 on growth and superoxide formation in *Vicia faba*. (A) *Vicia faba* seedlings 7 days post treatment with NaN_3. (B) NBT test to visualize differential localization of superoxide in the *Vicia* root after s NaN_3 treatment for 3 h. C, control; T1, 0.5 mM NaN_3; T2, 1 mM NaN_3. See Materials and Methods section for procedures.

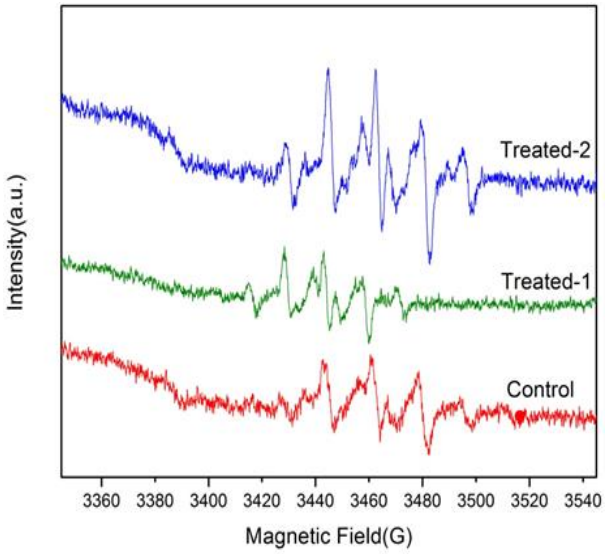

FIGURE 2. Formation of DMPO-radical adduct in *Vicia faba* treated with NaN_3. While the nature of the DMPO-radical adduct was unclear, NaN_3 at 1 mM (T2) caused an increased formation of the radical species as indicated by the increased height of the EPR spectral peaks, compared with control and 0.5 mM NaN_3 groups. See Materials and Methods section for procedures.

peak intensity in the treated groups as compared to the control. Increased free radicals were shown in T2 root tips, with intensified peaks clearly revealing generation of more hydroxyl free radicals in the group as compared to T1 and C. These alterations were supported by the reduced activity of catalase and superoxide dismutase in the treated plants.

3.3. Enzymatic Antioxidant Activity

The superoxide and H_2O_2 scavenging capacity were measured in the root cells of *Vicia* seedling by SOD and CAT activity assays, respectively. **Figure 3a** showed the effect of NaN_3 on the SOD activity in the root cells. A dose-dependent decrease in SOD activity was observed in treated groups as compared to control group. A significant ($p < 0.01$) decrease (44.86%) in SOD activity as compared to control was found in T2 groups. T1 also showed decreased SOD activity, but this decrease was found to be statistically insignificant when compared to the control. Similarly, CAT activity was also found to be reduced significantly in both treated groups. A significant decrease (61.69% and 49.20%) in CAT activity was observed in T2 and T1 groups, respectively, as compared to control. Furthermore, to find out the impact of the decreased activity of plant defense markers (SOD and CAT) on the cell membranes, the lipid-peroxidation product malondialdehyde (MDA) level was measured. MDA is a good marker of damage to the cell membranes. As shown in **Figure 3c**, the highest damage to the cell membranes was observed in T2 with a six-fold ($p < 0.01$) increase in MDA content as compared to control, whereas a non-significant increase was observed in T1 as compared to control.

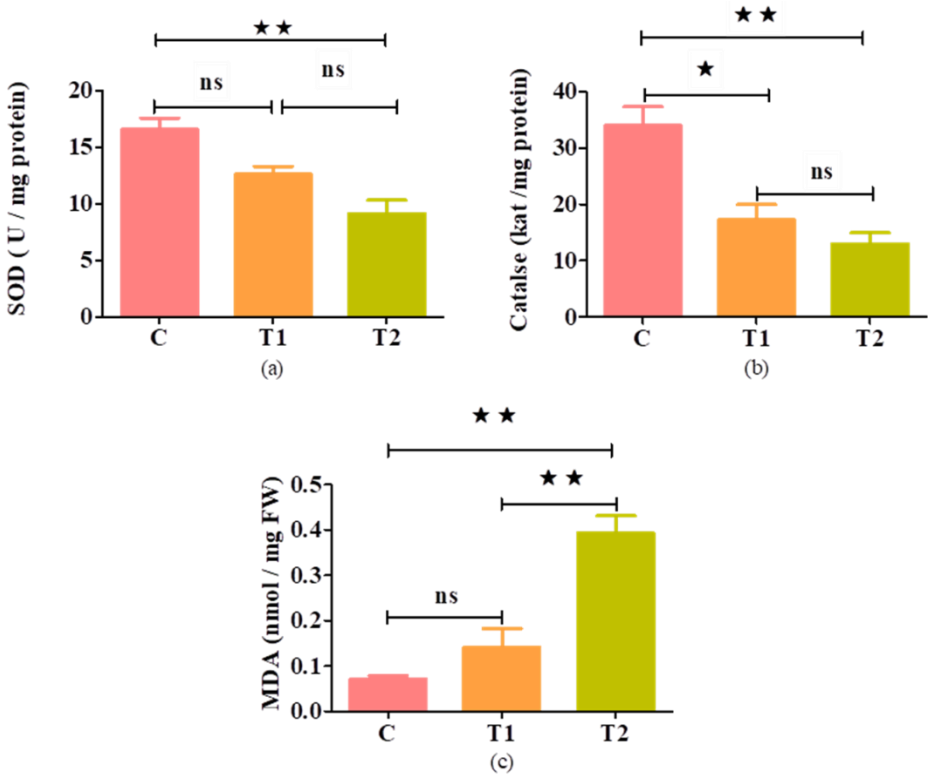

FIGURE 3. Effect of NaN_3 on SOD (a), CAT (b), and MDA content (c) in *Vicia faba*. Data represent mean ± standard error (n = 3). *, $p < 0.05$; **, $p < 0.01$; ns, no statistical significance. See Materials and Methods section for procedures.

3.4. Mitotic Index

The mitotic index (MI) was examined to monitor the effects of NaN_3 exposure to the plants on dividing capacity of the root cells. MI is represented by the percentage of dividing cells out of total cells observed. Supplemental **Figure S1** displayed a microscopic image of the dividing cells observed in the meristematic region of *Vicia faba* roots exposed to NaN_3. Decreased MI in T1 (74.33%) and T2 (60.63%) compared to control (88.23%) was observed, indicating that the higher dose (T2) hindered the cell division phenomenon more noticeably as compared to the lower dose (T1) and control.

3.5. Single-Cell Gel Electrophoresis

Genotoxicity of NaN_3 exposure of *Vicia faba* seedlings was assessed by single-cell gel electrophoresis (the comet assay). Supplemental **Figure S2** showed the comet formation of root tip nuclei of *Vicia faba* after exposure to NaN_3. As revealed in **Figure 4**, a very significant ($p < 0.001$) increase in comet olive moment (16.70 and 20.35) was found in T1 and T2, respectively, as compared to control (2.15). The results indicated that NaN_3 caused substantial DNA damage in the root cells.

4. DISCUSSION

In this investigation, we presented a brief account of the detection of even small quantity of oxygen free radicals in *Vicia faba* plants treated with NaN_3 and provided a rationale for using the EPR spin-trapping technique in such studies. The free radicals detected by EPR spectroscopy were further validated by comparative analysis of the results obtained with differ-

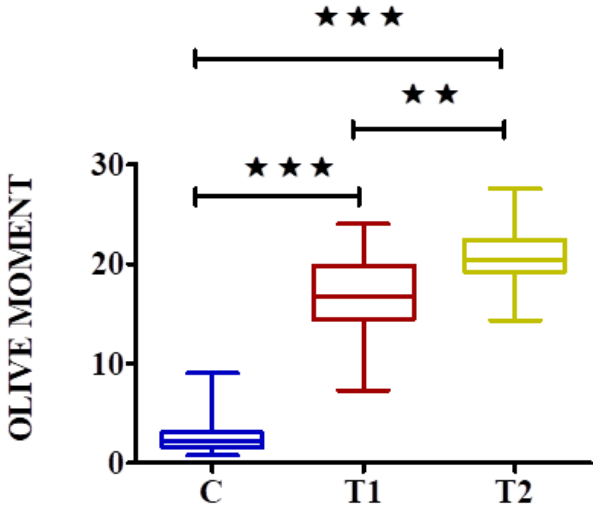

FIGURE 4. Olive moments obtained from the comet assay of the root tip nuclei of *Vicia faba* after exposure to NaN_3. The figure shows box plots of the olive moment of T1 and T2 against control C. Tail moments of 50 randomly selected comets are presented as quartile box plots. The edges of the box represent the 25th and the 75th percentiles; a solid line in the box represents the median. Error bars indicate 90th and 10th percentiles. The asterisk denotes the significant difference of the treated groups from the control group (nonparametric Kruskal Wallis test followed by Dunn's multiple comparison) for both data sets. **, $p < 0.01$; ***, $p < 0.001$; ns, no statistical significance. See Materials and Methods section for procedures.

ent conventional methods for free radical detection. NaN_3 is a chemical mutagen and used to enhance the quality, yield, and economy of plants. NaN_3 has been applied as a mutagen for breeding purposes to different plant parts including anther, in florescence, most commonly onto seeds at doses varying from 0.1 mM to 20 mM [10, 32, 33]. The toxicity of NaN_3 and most of its physiological effects can be traced to its reversible inhibitory effect on enzymes containing a coordinated divalent ion, such as those of cellular respiration, as well as its effects on the ROS mechanism [34]. Root tip is prone to free radical generation under stress conditions. Nutrient solutions for hydroponic culture are commonly maintained at a slightly low pH to facilitate better nutrient absorption. At the same time, NaN_3 also requires low pH to function as a mutagen. In the present study, two concentrations (0.5 and 1.0 mM) of NaN_3 solutions were prepared in ½ strength Hoagland nutrient solution which was previously maintained at 5.6 pH and applied to *Vicia faba* seedlings through their roots for a short period of time (24 h).

Due to the very short half-life of free radicals, DMPO is used as a spin trap to form relatively stable DMPO-radical adduct. Binding of DMPO with hydroxyl radical and superoxide was well described in the supplemental **Figure S3** [35]. The DMPO-radical specific EPR spectrum consists of six-line signals with two major signals having g value around 2.015 and 2.006 (peaks No. 2 and 4 in **Figure 2**). The middle prominent peak (peak No.4) in all three spectra (C, T1, and T2) having a g value of 2.006, represented the stress-generated DMPO-OH adduct. The DMPO-OH hyperfine splitting (providing detail account of a molecule, most often of radicals) of the spectrum of *Vicia faba* root cells of all the three groups (C, T1, and T2) was shown in **Figure 2**. The pattern of the spectra is similar to that previously reported by others [36, 37]. In the biological systems (plant and animal tissues), DMPO specifically reacts to radicals at double bonds. Due to interactions between the electron spins and the nuclear spins of atoms, specific EPR signal profiles and consequently, characteristic hyperfine structures are generated. The number of peaks resulting from the hyperfine splitting of radicals may be predicted by the following equations: No. of peaks (hyperfine) = 2 nI + 1 for atoms having one equivalent nuclei; No. of peaks (hyperfine) = (2 nI + 1) + (2 nI + 1) for atoms with multiple equivalent nuclei; where, n = No. of atom/electron and I = spin (spin for nitrogen =1, oxygen = 0, and carbon = 0).

Under the present condition, hyperfine splitting arises due to interaction between nitrogen and hydroxyl radicals. Thus, No. of peaks = (2 nI + 1) (2 nI + 1) = (2 x 1 + 1) for nitrogen center x (2 x 1/2 + 1) for $OH^{\cdot}$ center = 6.

Four initial peaks are due to nitrogen center of DMPO with two unpaired electrons (singlet) and last two peaks come from one unpaired electron of the hydroxyl free radicals. The branching of peaks indicates strong interaction and binding of unpaired electron with a central ion. The stronger the interactions between species, the more intensified peaks are obtained.

In the present study, growth of *Vicia* seedlings decreased with the increasing concentrations of NaN_3 (**Figure 1a**). These alterations were accompanied by the increased free radical generation and reduced SOD and CAT activity in T2 and T1 as compared to C. Due to the inhibitory effect of sodium azide on electron transport chain, adenosine triphosphate (ATP) synthesis is hindered which causes slowing down of several vital cellular processes. The reduced ATP synthesis might have resulted in the reduced mitotic index (MI) at the higher dose, i.e., 1 mM NaN_3. MI was also found to be 50% after 0.5% sodium azide treatment to *Trigonella foenum-graecum* seeds as described by Siddiqui et al. [38]. Similar results of declined mitotic activity in *Sesamum indicum* L. have been shown by Birara et al. [39]. SOD is one of the most effective intracellular enzymatic antioxidant, catalyzing the conversion of superoxide to dioxygen and hydrogen peroxide. Catalase is present in the peroxisome of aerobic cells and promotes the conversion of hydrogen peroxide to water and molecular oxygen [40–42]. Inhibitory effect of NaN_3 on SOD and CAT leads to accumulation of reactive superoxide, hydrogen peroxides (H_2O_2), and hydroxyl radicals [43–45]. Excessive H_2O_2 leads to irreversible oxidation of thiol/thiolate groups (more commonly cysteine residues) of proteins to sulfinic ($-SO_2H$) and sulfonic acids ($-SO_3H$) leading to the altered protein function [45]. Superoxide react with H_2O_2 via the Haber–Weiss reaction to generate highly reactive hydroxyl free radicals [44]. At the higher dose of NaN_3 a significant decrease in SOD and CAT activity as compared to control was obtained. Lack of superoxide and H_2O_2 scavengers in the cells provokes their accumulation and initiates a cascade of chain reactions with DNA, protein, and lipids leading to DNA strand breaks (depicted by the comet assay) and lipid peroxidation (determine by increased MDA content) in the root cells.

5. CONCLUSION

EPR spectroscopy is a very useful method for the direct detection of free radicals at concentrations as low as 1 µM. A free radical contains an unpaired electron(s) in its outer orbit. They are extremely reactive and easily take part in chemical reactions with vital cell components in the body. These reactions occur through a chain of oxidative reaction thereby causing tissue injury. ROS are the main cause of oxidative stress and responsible for causing damage to proteins, lipids, and DNA. Plant breeders, environmentalists, and toxicologists can use EPR spin trapping method to detect the ex-situ free radicals produced in biological samples and find a chance to weigh up the beneficial effects over the detrimental effects. Using this method via recording and quantifying free radicals non-invasively at any stages of growth, one can also get the early evidence of the lethal doses of various chemical mutagens, pesticides, herbicides, and other xenobiotic compounds on plants.

ACKNOWLEDGMENT

We acknowledge receipt of UGC Postdoctoral Fellowship from University Grant Commission, Government of India and extend thanks to the Advanced Instrumentation Research Facility (AIRF) supported by Department of Biotechnology (DBT) builder program, Jawaharlal Nehru University, New Delhi, for EPR facility.

REFERENCES

1. Wang Z, You R. Changes in wheat germination following gamma-ray irradiation: an in vivo electronic paramagnetic resonance spin-probe study. *Environ Exp Bot* 2000; 43(3):219–25.
2. Swartz HM, Berliner LJ. Introduction to in vivo EPR. In: Berliner LJ, editor. Biological magnetic resonance: In *Vivo EPR (ESR): Theory and Application* (LJ Berliner). Springer, Berlin, Germany. 2012, pp. 1–12.
3. Goodman BA. X-band electron paramagnetic resonance (EPR) spectroscopic investigations of free radical and other redox processes in whole plant tissues and in vivo: a review. *Burapha Sci J* 2015; 18:321–46.
4. Rohn S, Kroh LW. Electron spin resonance: a spectroscopic method for determining the antioxidative activity. *Mol Nutr Food Res* 2005; 49(10):898–907. doi: 10.1002/mnfr.200400102.
5. Karunakaran C. Solar photocatalytic disinfection of bacteria. In: New and Future Developments in Catalysis (S Suib). Elsevier, Amsterdam, Netherlands. 2013, pp. 243–56.

6. Hawkins CL, Davies MJ. Detection and characterisation of radicals in biological materials using EPR methodology. *Biochim Biophys Acta* 2014; 1840(2):708–21. doi: 10.1016/j.bbagen.2013.03.034.
7. Spasojevic I, Mojovic M, Ignjatovic A, Bacic G. The role of EPR spectroscopy in studies of the oxidative status of biological systems and the antioxidative properties of various compounds. *J Serb ChemSoc* 2011; 76:647–77.
8. Villamena FA, Zweier JL. Superoxide radical trapping and spin adduct decay of 5-tert-butoxycarbonyl-5-methyl-1-pyrroline N-oxide (BocMPO): kinetics and theoretical analysis. *J Chem Soc, Perkin Trans 2* 2002; 7:1340–4.
9. Kelley WD, Rodriguez-Kabana R. Effects of annual applications of sodium azide on soil fungal populations with emphasis on *Trichoderma* species. *Pestic Sci* 1981; 12:235–44.
10. Olsen O, Wang X, von Wettstein D. Sodium azide mutagenesis: preferential generation of A.T→G.C transitions in the barley Ant18 gene. *Proc Natl Acad Sci USA* 1993; 90(17):8043–7.
11. Al-Qurainy F, Khan S. Mutagenic effects of sodium azide and its application in crop improvement. *World Appl Sci J* 2009; 6:1589–601.
12. Kochanova Z, Razna K, Zuriaga E, Badenes M, Brindza J. Sodium azide induced morphological and molecular changes in Persimmon (*Diospyros Lotus L.*). *Agriculture* 2012; 58:57–64.
13. Animasaun DA, Oyedeji S, Azeez MA, Onasanya AO. Alkylating efficiency of sodium azide on pod yield, nut size and nutrition composition of Samnut 10 and Samnut 20 varieties of groundnut (*Arachis hypogea L.*). *Afr J Food Agric Nutr Dev* 2014; 14:9497–510.
14. Abdulrazaq A, Ammar K. Effect of the chemical mutagens sodium azide on plant regeneration of two tomato cultivars under salinity stress condition in vitro. *Journal of Life Sciences* 2015; 9:27–3.
15. Owais WM, Kleinhofs A. Metabolic activation of the mutagen azide in biological systems. *Mutat Res* 1988; 197(2):313–23.
16. Somers DA, Anderson PC. In vitro selection for herbicide tolerance in maize. In: *Biotechnology in Agriculture and Forestry 25: Maize* (YPS Bajaj). Springer, Berlin, Germany. 1994, pp. 293–313.
17. Gruszka D, Szarejko I, Maluszynski M. Sodium azide as a mutagen. In: Plant Mutation Breeding and Biotechnology (QY, Shu, BP Forster, H Nakagawa). CABI, Wallingford, UK. 2012, pp. 159.
18. Leary SC, Hill BC, Lyons CN, Carlson CG, Michaud D, Kraft CS, et al. Chronic treatment with azide in situ leads to an irreversible loss of cytochrome c oxidase activity via holoenzyme dissociation. *J Biol Chem* 2002; 277(13):11321–8. doi: 10.1074/jbc.M112303200.
19. Kanaya N, Gill BS, Grover IS, Murin A, Osiecka R, Sandhu SS, et al. *Vicia faba* chromosomal aberration assay. *Mutat Res* 1994; 310(2):231–47.
20. Ma TH, Cabrera GL, Owens E. Genotoxic agents detected by plant bioassays. *Rev Environ Health* 2005; 20(1):1–13.
21. Grant WF, Owens ET. Zea mays assays of chemical/radiation genotoxicity for the study of environmental mutagens. *Mutat Res* 2006; 613(1):17–64. doi: 10.1016/j.mrrev.2006.04.002.
22. Patlolla KA. Environmental toxicity monitoring of nanomaterials using *Vicia faba* GENE-TOX assay. *J Nanomed Nanotech* 2013, 4:e129. doi: 10.4172/2157-7439.1000e129.
23. O'Sullivan DM, Angra D. Advances in Faba bean genetics and genomics. *Front Genet* 2016; 7:150. doi: 10.3389/fgene.2016.00150.
24. Del Carmen Cordoba-Pedregosa M, Cordoba F, Villalba JM, Gonzalez-Reyes JA. Zonal changes in ascorbate and hydrogen peroxide contents, peroxidase, and ascorbate-related enzyme activities in onion roots. *Plant Physiol* 2003; 131(2):697–706. doi: 10.1104/pp.012682.
25. Giannopolitis CN, Ries SK. Superoxide dismutases: I. Occurrence in higher plants. *Plant Physiol* 1977; 59(2):309–14.
26. Beauchamp C, Fridovich I. Superoxide dismutase: improved assays and an assay applicable to acrylamide gels. *Anal Biochem* 1971; 44(1):276–87.
27. Bradford MM. A rapid and sensitive method for the quantitation of microgram quantities of protein utilizing the principle of protein-dye binding. *Anal Biochem* 1976; 72:248–54.
28. Sinha AK. Colorimetric assay of catalase. *Anal Biochem* 1972; 47(2):389–94.
29. Dhindsa RS, Plumb-Dhindsa PL, Reid DM. Leaf

senescence and lipid peroxidation: effects of some phytohormones, and scavengers of free radicals and singlet oxygen. *Physiologia Plantarum* 1982; 56:453–7.
30. Gichner T, Plewa MJ. Induction of somatic DNA damage as measured by single cell gel electrophoresis and point mutation in leaves of tobacco plants. *Mutat Res* 1998; 401(1–2):143–52.
31. Galbraith DW, Harkins KR, Maddox JM, Ayres NM, Sharma DP, Firoozabady E. Rapid flow cytometric analysis of the cell cycle in intact plant tissues. *Science* 1983; 220(4601):1049–51. doi: 10.1126/science.220.4601.1049.
32. Castillo AM, Cistue L, Valles MP, Sanz JM, Romagosa I, Molina-Cano JL. Efficient production of androgenic doubled-haploid mutants in barley by the application of sodium azide to anther and microspore cultures. *Plant Cell Rep* 2011; 20:105–11.
33. Till BJ, Cooper J, Tai TH, Colowit P, Greene EA, Henikoff S, et al. Discovery of chemically induced mutations in rice by TILLING. *BMC Plant Biol* 2007; 7:19. doi: 10.1186/1471-2229-7-19.
34. Mashenkov A. Induced mutation process as a source of new mutants. *Maize Genetics Cooperation Newsletter* 1986; 60:70–1.
35. Santos ABD, Silva DHS, Bolzani VDS, Santos LA, Schmidt TM, Baffa O. Antioxidant properties of plant extracts: an EPR and DFT comparative study of the reaction with DPPH, TEMPOL and spin trap DMPO. *J Braz Chem Soc* 2009; 20:1483–92.
36. Harbour JR, Chow V, Bolton JR. An electron spin resonance study of the spin adducts of OH and HO_2 radicals with nitrones in the ultraviolet photolysis of aqueous hydrogen peroxide solutions. *Can J Chem* 1974; 52:3549–53.
37. Del Rio LA, Fernandez VM, Ruperez FL, Sandalio LM, Palma JM. NADH induces the generation of superoxide radicals in leaf peroxisomes. *Plant Physiol* 1989; 89(3):728–31.
38. Siddiqui S, Meghvansi MK, Hasan Z. Cytogenetic changes induced by sodium azide (NaN_3) on *Trigonellafoenum-graecum L*. seeds. *S Afr J Bot* 2007; 73:632–5.
39. Birara A, Muthuswarny M, Andargie M. Effect of chemical mutation by sodium azide on quantitative traits variations in *Sesamum indicum L*. *Asian J Biol Sci* 2013; 6:356–62.
40. Rahman K. Studies on free radicals, antioxidants, and co-factors. *Clin Interv Aging* 2007; 2(2):219–36.
41. Raja V, Majeed U, Kang H, Andrabi KI, John R. Abiotic stress: interplay between ROS, hormones and MAPKs. *Environ Exp Bot* 2017; 137:142–57.
42. Chojak-Kozniewska J, Linkiewicz A, Sowa S, Radzioch MA, Kuzniak E. Interactive effects of salt stress and Pseudomonas syringae pv lachrymans infection in cucumber: involvement of antioxidant enzymes, abscisic acid and salicylic acid. *Environ Exp Bot* 2017; 136:9–20.
43. Vidhyasekaran P. *Fungal Pathogenesis in Plants and Crops: Molecular Biology and Host Defense Mechanisms*. CRC Press, Boca Raton, FL, USA. 2007.
44. Demidchik V. Reactive oxygen species and oxidative stress in plants. In: Plant Stress Physiology (S Shabala). CAB International, O xford, UK. 2012, pp. 24–58.
45. Lennicke C, Rahn J, Lichtenfels R, Wessjohann LA, Seliger B. Hydrogen peroxide: production, fate and role in redox signaling of tumor cells. *Cell Commun Signal* 2015; 13:39. doi: 10.1186/s12964-015-0118-6.